

Relationship between Crystallite Size and Bond Lengths in Boehmite

X. Bokhimi,^{*,†,1} J. A. Toledo-Antonio,^{*} M. L. Guzmán-Castillo,^{*} and F. Hernández-Beltrán^{*}

^{*}Instituto Mexicano del Petróleo, Eje Central L. Cárdenas 152, A.P. 14-805, 07730 México, DF, Mexico; and [†]Institute of Physics, The National University of Mexico (UNAM), A.P. 20-364, 01000 México, DF, Mexico

Received November 16, 2000; in revised form January 17, 2001; accepted February 9, 2001; published online May 11, 2001

Boehmite with a crystallite size between 1 and 27 nm was prepared by annealing a boehmite precipitate under hydrothermal conditions at different temperatures. The crystalline structure, measured with X-ray powder diffraction, was refined with the Rietveld method. From the refinement bond lengths and bond angles between oxygen and aluminum atoms were calculated, which revealed that boehmite bond lengths and local symmetry depended on crystal dimensions. When boehmite's crystallite size decreased, Al–OH interaction increased, and the local octahedral symmetry tended to be tetrahedral. The hydrogen bond, sustaining boehmite's crystalline structure, and the bonds between oxygen atoms and hydroxyls inside the octahedra double layers, building the crystalline structure, became weaker as crystallite size decreased, which could explain why boehmite's transformation temperature into a transitional alumina also decreased with crystallite size. Alumina crystallite size also depended of the corresponding size of boehmite. It was shown that desorbed water from annealed samples came from the crystal surface and not from the bulk. © 2001 Academic Press

Key Words: Boehmite's crystallography; Rietveld refinement; bond lengths; crystal's surface; transitional alumina.

INTRODUCTION

Aluminum oxide is widely used in industry, for example, for refining petroleum (1–4), as a substrate in integrated circuits (5), or for reducing pollution (6). Considering atom ordering in its crystalline structure, this oxide can be classified into two groups: the one represented by alpha alumina with its atoms in a hexagonal arrangement (7) and the group of the transitional aluminas (χ -, η -, γ -, κ -, and θ -alumina), where atoms are ordered in a spinel-based structure (8). Alpha alumina, which is free of hydroxyls, is the most stable phase and is obtained after annealing samples at temperatures higher than 800°C. The crystalline structure of transitional aluminas, which are characterized by containing hydroxyls in its structure, has been only approximated

(9), the reported models only provide a first idea about real atomic ordering. The most recent report about the crystalline structure of these aluminas corresponds to the theta phase (10), which, however, is only a new approximation but not the correct solution.

Aluminas are commonly obtained from four precursors: two hydroxides, gibbsite (11) and bayerite (12); and two oxyhydroxides, diaspore (13) and boehmite. Although this last phase has been widely used for preparing aluminas, a detailed characterization of boehmite is lacking. In literature boehmite is classified in two big groups: the one where the samples are well crystallized and the named pseudoboehmite group (14). Recently we have suggested that boehmite and pseudoboehmite represent the same phase but with different crystallite size (15). In order to provide more evidence to justify this proposition, we have prepared boehmite samples with well-defined and controlled crystallite size and have analyzed in detail the corresponding crystallography.

When boehmite is the precursor for alumina synthesis, its characteristics determine crystal and particle properties of the synthesized transitional and alpha aluminas; for example, sintering and transformation temperatures and their thermal stability. The transformation temperature of boehmite into a transitional alumina (16) and of θ - into α -alumina (17) increases as boehmite crystallite size increases; the origin of this temperature dependence, however, has not been explained. It could be associated to changes in atom bonds, because detailed studies in natural and synthetic boehmite show different bond lengths in both systems (18, 19).

In order to understand boehmite properties in more detail, we have prepared it with different crystallite sizes by growing a boehmite precipitate under hydrothermal condition at different temperatures and have refined the crystalline structure with the Rietveld method, starting from X-ray powder diffraction patterns. From the refinement we calculated bond lengths and bond angles between oxygen and aluminum atoms. Since it was possible to prepare boehmite with crystallite sizes between 1 and 27 nm, the present study suggests a possible behavior of atoms near boehmite's surface.

¹To whom correspondence should be addressed. E-mail: bokhimi@fenix.ifisicacu.unam.mx.

EXPERIMENTAL

Synthesis. Boehmite crystal growth was performed under hydrothermal conditions. Seeds were precipitated at room temperature (23°C) by mixing, dropwise on 50 mL of distilled water at pH 8, an aqueous solution of aluminum complex ions and a solution rich in hydroxyls. The first solution (300 mL, 0.3 M Al^{3+}) was prepared from $\text{AlCl}_3 \cdot 6\text{H}_2\text{O}$ (J. T. Baker) and distilled water; the second one (100 mL) from NH_4OH (J. T. Baker, 50 vol%). The suspension (450 mL) with the boehmite precipitate was placed in a 600-mL autoclave and heated and stirred at a fixed temperature between 23 and 240°C for 18 h under autogenous pressure. Thereafter, it was filtered and washed thoroughly with distilled water until it was chlorine free (silver nitrate test), and dried overnight at 110°C in air.

Characterization. X-ray diffraction patterns of the samples packed in a glass holder were recorded at room temperature with $\text{CuK}\alpha$ radiation in a Bruker Advance D-8 diffractometer having theta–theta configuration and a graphite secondary-beam monochromator. Diffraction intensity was measured by step scanning in the 2θ range between 10° and 127°, with a 2θ step of 0.02° for 8 s per point. Crystalline structures were refined with the Rietveld technique by using DBWS-9411 (20) and FULLPROF-V3.5d (21) codes; peak profiles modeled with a pseudo-Voigt function (22) contained average crystallite size as one of its characteristic parameters (23). Standard deviations, which show the last figure variation of a number, are given in parentheses; when they correspond to refined parameters, their values are not estimates of the probable error in the analysis as a whole, but only of the minimum possible probable errors based on their normal distribution (24).

RESULTS AND DISCUSSION

Crystallography and Crystal Morphology

All fresh samples contained only boehmite. Its crystalline structure was refined by modeling it with an orthorhombic unit cell having atoms in the positions given in Tables 1 and 2, and the symmetry described by space group *Cmcm*. Until now, this is the best model reported for boehmite's crystalline structure (25). In Table 1, O1 corresponds to the position of oxygen atoms shared by four octahedra, and O2 represent the position of oxygen atoms of hydroxyls, which participate in the hydrogen bonding that sustain boehmite's crystalline structure (Fig. 1).

For a given sample, the peak widths of its diffraction pattern were so different (Figs. 2 and 3) that they could not be explained by only considering strain and crystallite size effects; the widest peak corresponded to (020) reflection. This width difference was an effect of crystal form anisotropy, because they are platelet-like, as observed by high-

TABLE 1
Boehmite, Space Group *Cmcm*: Atom Fractional Coordinates

Atom	Site	x	y	z
Al	4c	0.0	y_{Al}	0.25
O1	4c	0.0	y_{O1}	0.25
O2	4c	0.0	y_{O2}	0.25

Note. Since hydrogen X-ray diffraction is negligible, it was not considered.

resolution electron microscopy (26). For the refinement, this form anisotropy was modeled by using FULLPROF code (21), which showed that crystals grew with their plates parallel to (020) planes. The only adjustment coefficients used for the refinement where the four defining the polynomial to model background. For the samples with large crystallites, 32 independent variables were used; this number was reduced to 17 for the samples with small crystallites, because the anisotropic temperature factors were fixed. Two more constrains were used in the refinement of all samples: The *V* and *W* parameters associated to the gaussian contribution of the peak profile were fixed to their values determined from the refinement of standard samples with large crystallites. Figure 4 displays a typical Rietveld refinement plot.

For all samples the crystal shortest dimension was the one parallel to [020] direction, which for boehmite's crystalline structure is perpendicular to [020] planes. This property can be explained by analyzing the crystalline structure made of oxygen octahedra with aluminum atom near their centers and oxygen atoms in their vertices (Fig. 5); two of the oxygen atoms belong to hydroxyl ions. Octahedra form double layers perpendicular to *b* axis (Fig. 1) that interact between each other via an hydrogen bonding $\text{OH} \cdots \text{O}$; this kind of bond has typical bond energies about 20 kJ/mol (27). In the present case, this bonding is destroyed between 300 and 550°C, which is the temperature range where boehmite is transformed into a transitional alumina. Detailed

TABLE 2
Atom Fractional Coordinate *y* of Atoms for the Different Heating Temperatures

<i>T</i> (°C)	y_{Al}	y_{O1}	y_{O2}
23	−0.3239(3)	0.3100(5)	0.0841(4)
30	−0.3238(3)	0.3104(5)	0.0843(4)
50	−0.3247(3)	0.3043(4)	0.0860(3)
100	−0.3227(3)	0.2982(4)	0.0856(4)
140	−0.3192(2)	0.2927(4)	0.0780(3)
180	−0.3182(2)	0.2907(3)	0.0797(2)
240	−0.3180(1)	0.2905(2)	0.0795(2)

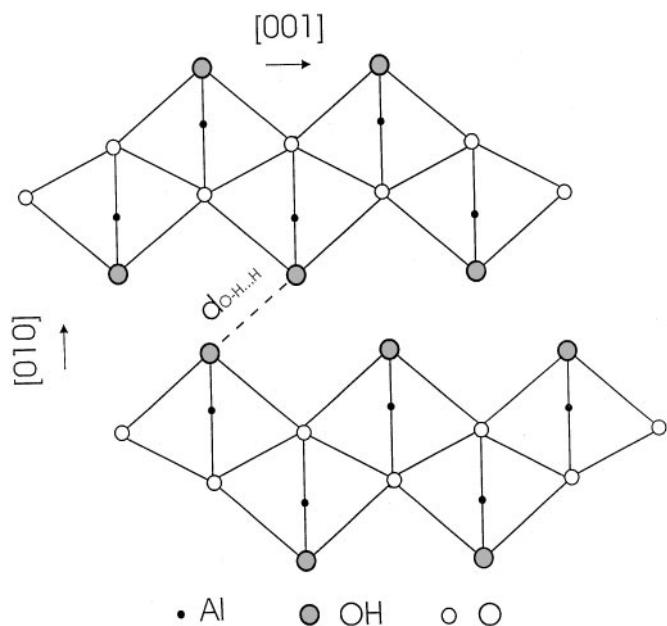


FIG. 1. Projection of boehmite crystalline structure perpendicular to the a axis. The hydrogen bonding between the double layers is shown.

information (covalent O–H and electrostatic O–H...O bond lengths) about this boehmite bonding is reported for neutron diffraction experiments (25); it is similar to those

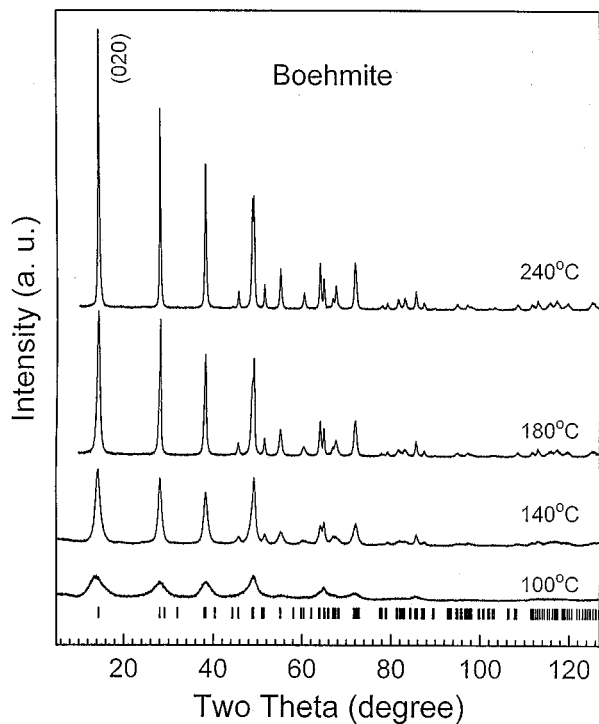


FIG. 2. X-ray diffraction patterns of the samples heated under hydrothermal conditions at temperatures between 100 and 240°C. Tick marks correspond to boehmite; the Miller indices, (020), of the first peak are also shown.

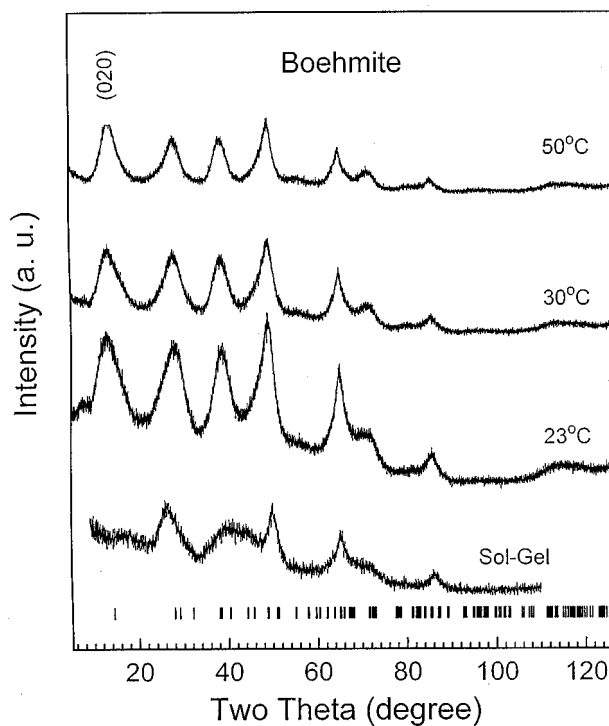


FIG. 3. X-ray diffraction patterns of samples heated under hydrothermal conditions at temperatures between 23 and 50°C and the one prepared via sol-gel technique. Tick marks correspond to boehmite; the Miller indices, (020), of the first peak are shown.

published for its isomorphous phase, lepidocrocite (γ -FeOOH), which has been also characterized with neutron diffraction (28,29). The discussion in the next paragraphs about bond lengths in the basic octahedra (Fig. 5) will make

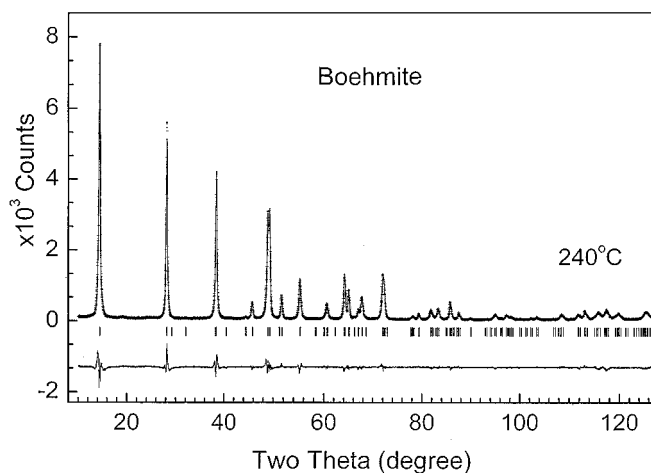


FIG. 4. Rietveld refinement plot of the sample heated at 240°C ($R_{wp} = 0.145$). Circles correspond to the experimental data, and the continuous line to the calculated one. Tick marks represent boehmite ($R_{Bragg} = 0.028$).

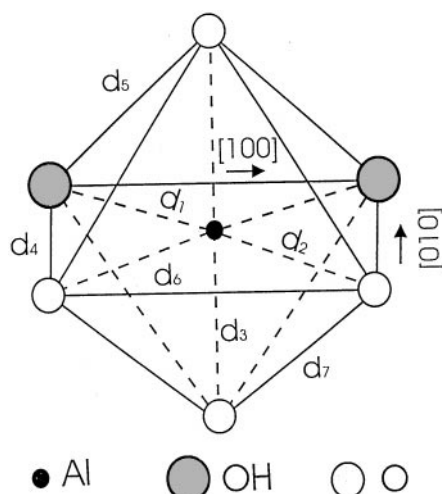


FIG. 5. Octahedron representative of boehmite crystalline structure.

evident why boehmite crystals grow mainly along the a - c plane, where atomic bonds are stronger than interlayer hydrogen bonds.

Crystallite Dimensions

Boehmite crystallite dimensions depended on the heating temperature for the hydrothermal treatment (Table 3): Crystallite thickness varied from 26.3(5) nm for the samples treated at 240°C to the dimensions of a unit cell, 1.13(1) nm, for those treated at 23°C. It is worth mentioning that boehmite prepared with the sol-gel technique can have a “crystallite” thickness smaller than a unit cell (30), as it is concluded from the absence of (020) reflection peak in the X-ray diffraction pattern (Fig. 3). For the used hydrothermal conditions, large heating times produced only small thickness increases; for example, in the boehmite heated at 240°C, crystallite thickness grew from 26.5(3) to 34.3(3) nm when heating time varied from 18 to 138 h.

Crystallite dimension along plates also grew as heating temperature was increased (Table 3): for 23°C it was

TABLE 3
Boehmite Crystallite Dimensions for the Different Heating Temperatures

T (°C)	$d_{(020)}$ (nm)	$d_{(200)} = d_{(002)}$ (nm)
23	1.13(1)	3.21(8)
30	1.56(2)	3.53(8)
50	2.04(4)	4.0(1)
100	2.42(4)	5.4(1)
140	6.90(8)	16.6(4)
180	14.2(2)	43(2)
240	26.3(5)	49(1)

TABLE 4
Boehmite Lattice Parameters as a Function of Crystallite Size

$d_{(020)}$ (nm)	a (nm)	b (nm)	c (nm)
1.13(1)	0.2851(1)	1.212(1)	0.3736(1)
1.56(2)	0.28796(8)	1.2205(9)	0.3761(1)
2.04(4)	0.28675(9)	1.2274(9)	0.3733(1)
2.42(4)	0.28686(9)	1.2265(9)	0.3715(1)
6.90(8)	0.28695(3)	1.2232(2)	0.36945(4)
14.2(2)	0.28681(1)	1.22256(8)	0.36941(2)
26.3(5)	0.28678(1)	1.22188(4)	0.36941(4)

3.21(8) nm and for 240°C it was 49(1) nm. The smallest dimension on these plates, 3.21(8) nm, however, was nearly 10 times the unit cell dimension along them (Table 4), indicating that boehmite crystals grew with preference along plates. This fact was more spectacular in sol-gel samples (30); in this case, diffraction patterns showed only the reflections associated to these dimensions (Fig. 3). Because in the present work crystallite thickness is representative of crystallite size, in the rest of the discussion this thickness will be used to represent crystallite size when its effect on parameters will be discussed.

Boehmite crystallite growing under hydrothermal conditions was similar to the one reported for other compounds grown with the same method (31): crystallite size increases when heating temperature is increased. This size can also be increased by changing the solvent or the mineralizer in the hydrothermal treating (32, 31).

Atom Bond Lengths

The octahedra building boehmite double layers are oriented parallel to unit cell axis. Along the c axis, octahedra share vertices (Fig. 1), and along the a axis they share their edges parallel to the b axis (Fig. 6); in this way, each oxygen atom (not belonging to hydroxyls) is shared by four octahedra. In contrast, the oxygen atom of hydroxyls is only shared by two octahedra (Figs. 1 and 6). This reveals that the interactions along the a - c plane, given by the interaction between the oxygen atoms shared by four octahedra and aluminum atoms, should be stronger than the interaction between two octahedra double layers, favoring crystal growing along planes and not perpendicular to them.

Lattice parameters a and b were almost independent on boehmite’s crystallite size (Table 4); in contrast the lattice parameter c increased as crystallite size diminished. This result is useful in proposing a model for the atom behavior near boehmite’s crystal surface. As it will be evident from the discussion below, when the crystallite size decreases the expansion along c axis is related to stronger interactions between aluminum and oxygen atoms participating in hydrogen bonding.

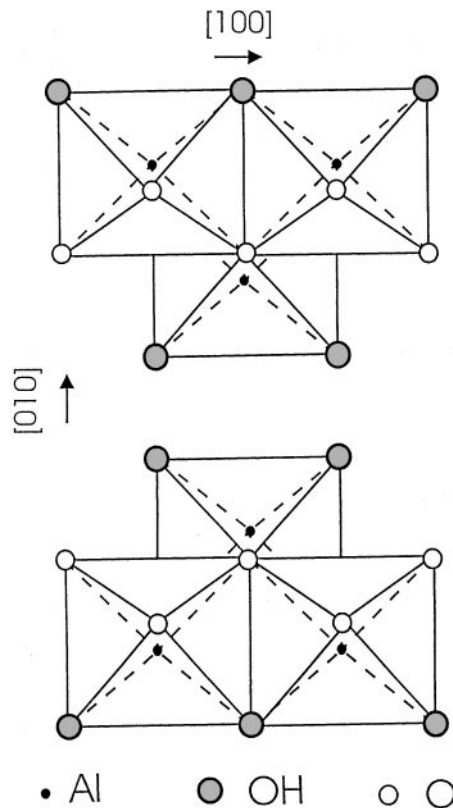


FIG. 6. Projection of boehmite crystalline structure along the [001] direction.

To understand more about boehmite's behavior, we calculated some characteristic atom bond lengths and atom bond angles in the octahedron representative of its crystalline structure (Fig. 5). If readers are interested in other distances and angles different to those listed in the tables, the information about boehmite crystallography we are providing in the present work is enough to do it. To avoid misunderstandings, we will clearly define the different distances and angles reported in tables and figures (Tables 5 through 7 and Figs. 1 and 5 through 7). The bond length between an aluminum atom and the oxygen of hydroxyl (Al–OH) is named d_1 ; d_2 is the bond length between aluminum and oxygen atoms (Al–O) in the octahedra's plane defined by hydroxyls and aluminum atoms (HO–Al–OH). The bond length between aluminum and oxygen atoms in an octahedron vertex that is outside of the HO–Al–OH plane (along text, this oxygen will be named as the oxygen in octahedron vertex) corresponds to d_3 ; d_4 is the bond length between oxygen and hydroxyls in HO–Al–OH plane, while d_5 is the bond length between hydroxyl and the oxygen in the octahedron vertex. The bond length between oxygen atoms in the plane HO–Al–OH is designated by d_6 , which is equal to the bond length between hydroxyls in the same plane; the bond length between oxygen atoms in and outside

TABLE 5
Bond Lengths as a Function of Boehmite Crystallite Size

$d_{(020)}$ (nm)	d_1 (nm)	d_2 (nm)	d_3 (nm)	d_4 (nm)
1.13(1)	0.1810(1)	0.2160(1)	0.18756(6)	0.2738(2)
1.56(2)	0.1825(1)	0.2181(1)	0.18876(6)	0.2760(2)
2.04(4)	0.1805(1)	0.2136(1)	0.18832(6)	0.2680(2)
2.42(4)	0.1823(1)	0.2063(1)	0.18815(6)	0.2607(2)
6.90(8)	0.1892(1)	0.1983(1)	0.18755(6)	0.2602(2)
14.2(2)	0.1901(1)	0.1957(1)	0.18774(6)	0.2580(2)
26.3(5)	0.1904(1)	0.1953(1)	0.18774(6)	0.2578(2)

of the HO–Al–OH plane correspond to d_7 . Finally, the hydrogen bond length between contiguous octahedra double layers is named $d_{\text{OH}\dots\text{O}}$ (Fig. 1). The angle between an aluminum atom and the two next neighboring hydroxyls bonds in the plane HO–Al–OH (Fig. 7a) was represented with Greek letter δ . The angle in the same plane between the aluminum atom and the hydroxyl and oxygen atom bonds in the quasi-diagonal was represented with η (Fig. 7b). The angle formed by the interaction between aluminum atom and the oxygen atoms in vertices was represented with ϕ (Fig. 7c).

The bond lengths between the aluminum and oxygen of hydroxyls and the oxygen in the HO–Al–OH plane, d_1 and d_2 , respectively (Figs. 5 and 7 and Table 5), tended to be equal for large crystal dimensions. Since in the present work the thickest crystals were only 26.3(5) nm, it is expected that for boehmite microcrystals both bond lengths to be equal. This and the fact that the angle η between these bonds (Table 5) moved to 180° as this thickness increased suggest that the orthorhombic symmetry of boehmite unit cell would probably change to a tetragonal symmetry for microcrystals.

When boehmite crystallite dimensions diminished, the interaction between aluminum atom and hydroxyls was stronger, producing shorter Al–OH bond lengths and larger δ angles between them (Table 6); this angle moved from $97.73(6)$ for the largest crystal thickness, 26.3(5) nm, to the

TABLE 6
Some Bond Angles (Fig. 7) in the Representative Octahedron as a Function of Boehmite Crystallite Size

$d_{(020)}$ (nm)	ϕ	η	δ
1.13(1)	169.69(3)	190.68(6)	103.93(6)
1.56(2)	170.06(3)	190.74(6)	104.16(6)
2.04(4)	164.72(3)	190.44(6)	105.20(6)
2.42(4)	161.62(3)	187.85(6)	103.80(6)
6.90(8)	160.10(3)	182.98(6)	98.65(6)
14.2(2)	159.37(3)	181.84(6)	97.93(6)
26.3(5)	159.38(3)	181.62(6)	97.73(6)

TABLE 7
Bond Lengths as a Function of Boehmite Crystallite Size

$d_{(020)}$ (nm)	d_5 (nm)	d_6 (nm)	d_7 (nm)	$d_{\text{O-H...O}}$ (nm)
1.13(1)	0.2677(1)	0.28510(4)	0.2763(1)	0.2765(1)
1.56(2)	0.2695(1)	0.28796(4)	0.2790(1)	0.2788(1)
2.04(4)	0.2712(1)	0.28675(4)	0.2705(2)	0.2818(1)
2.42(4)	0.2746(1)	0.28686(4)	0.26277(9)	0.2803(1)
6.90(8)	0.2810(1)	0.28695(4)	0.25616(8)	0.2691(1)
14.2(2)	0.2825(1)	0.28681(4)	0.25414(8)	0.2685(1)
26.3(5)	0.2827(1)	0.28677(4)	0.25391(8)	0.2681(1)

ideal angle (109.5°) for the small crystallites, which corresponds to a tetrahedral symmetry. It is worth commenting that the bond lengths of the small crystallites could be representative of their values on boehmite crystals surface of any dimension. If this is true, the kind of study reported in the present paper could be done in any system, and the

methodology used here represents an alternative method for studying the surface properties of solids, especially their crystallography.

The oxygen atoms not associated to hydroxyls interact with four aluminum atoms: two of them in the HO-Al-OH planes of edge-sharing octahedra (Figs. 5 and 6), and the other two belonging to vertex-sharing octahedra (Figs. 1 and 5). The bond length (d_2) associated to the interaction of aluminum atom with oxygen atom O1 in the HO-Al-OH plane decreased when the boehmite dimensions increased (Table 5); the bond length, d_3 , representing the interaction of aluminum atom with the oxygen atom O1 outside of this plane, however, was shorter and independent of boehmite crystal dimensions (Table 5). That means that the interaction along the [001] direction between oxygen and aluminum atoms (Fig. 7c) is stronger, and therefore, it will predominate during crystal growing. Consequently, crystals first grow along this direction, explaining the observed preferential crystal growing along plates. The above results

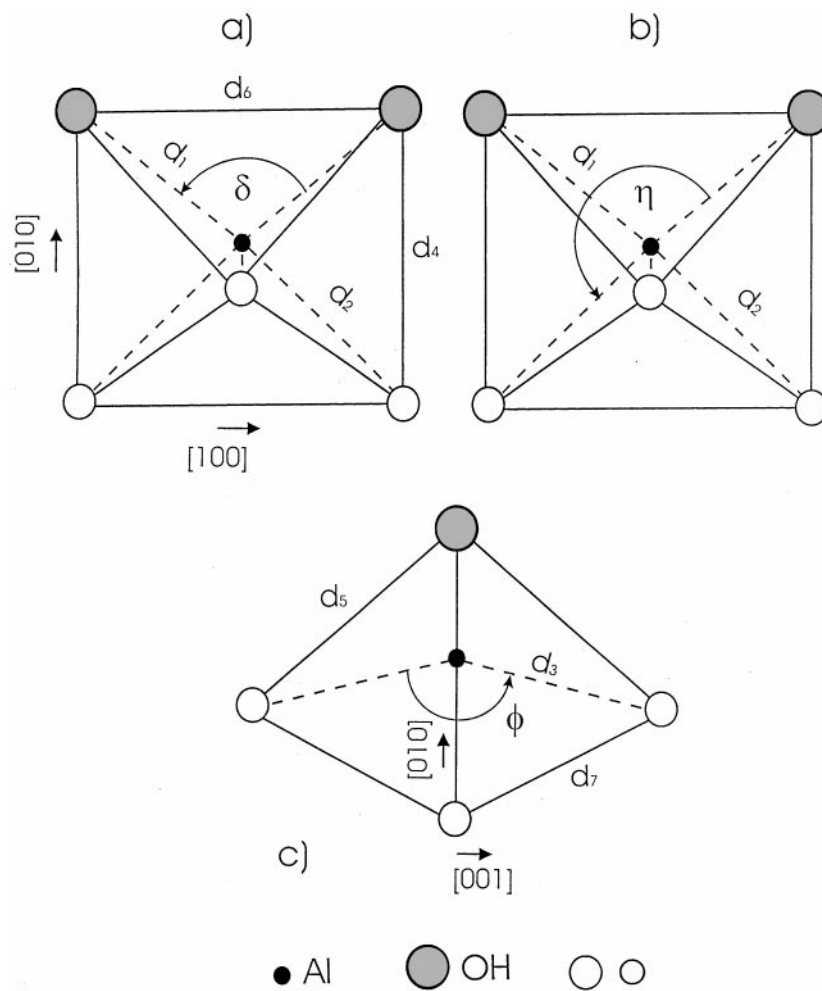


FIG. 7. Projections of the representative octahedron in order to detail bond lengths and bond angles: (a) and (b) along the [001] direction, (c) along the [100] direction.

also suggest that plate dimension along the c axis should be longer as observed by electron microscopy (26). This also explains why in the present study, the (002) peak of the diffraction pattern could not be fitted well (Fig. 4). The corresponding calculated peak was always broader than the experimental one, because the software used in the refinement assumes that crystal dimensions along the [100] and [001] directions are equal.

It is interesting to note that for the thickest crystal bond lengths d_4 and d_7 , between the oxygen in the HO–Al–OH plane and the oxygen of hydroxyls and oxygen in the vertex respectively were notoriously shorter than the corresponding length of the hydrogen bond between octahedra double layers (Figs. 4 and 5 and Tables 5 and 7); this differences were larger than 0.01 nm. This strong interaction causes octahedra deformation in direction to the center of the octahedra double layer (Fig. 8a). The shortness of these lengths suggests the possible existence of hydrogen bonds between these oxygen atoms; therefore, the hydrogen bond traditionally thought to occur in boehmite's crystalline structure needs to be revised. This analysis should be done via neutron diffraction in samples with large crystals. Bond lengths d_4 and d_7 increased as crystallite size diminished (Table 5), indicating a weaker interaction between the corresponding oxygen atoms, which increased octahedra symmetry around the c axis (Fig. 8b).

Water Adsorption

The crystallography results of the present analysis question the claim that water is intercalated between boehmite octahedra double layers (32) and extend the fact that water from samples with small crystallite size comes from crystallites surface (33). By correlating the maximum position of (020) reflection with the amount of water retained in the samples as a function of boehmite crystallite size, Lippens concluded that, like in other silicates (34), water was interca-

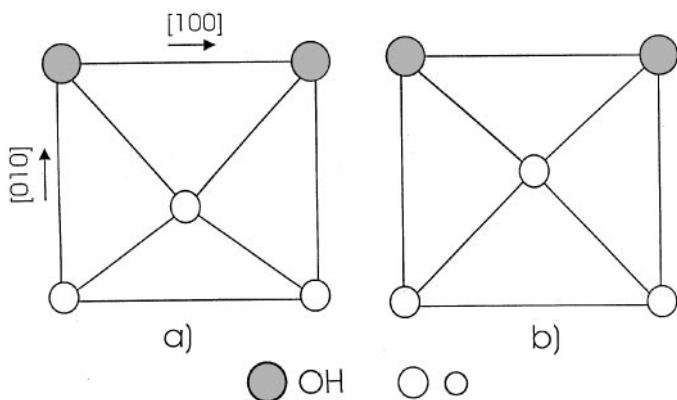


FIG. 8. Projection of the representative octahedra along the [001] direction: (a) for the sample heated at 240°C (large crystallite size); (b) for the one heated at 50°C (small crystallite size).

lated between boehmite octahedral double layers. Lippens (32) and Baker *et al.* (33) based their analysis on only the (020) reflection of the diffraction pattern (Baker correlated X-ray powder diffraction with NMR experiments). This kind of analysis with only one diffraction peak gives many degrees of freedom when models for the crystalline structure are constructed. The Rietveld refinement, however, is a full pattern analysis technique, and any proposed model for the crystalline structure must be compatible with all observed diffraction peaks; therefore, any model derived from this kind of analysis will be more realistic than those derived from the information involved in only one diffraction peak. In the present work, we observed a maximal variation of b lattice parameter of 0.005 nm between the samples with average crystallite size of 26.3(5) and those with crystallite size of 2.04 nm. This variation is 16 times smaller than the one reported by Lippens (32), which was 0.08 nm. Considering this small b lattice variation, it is impossible to intercalate water molecules between octahedra double layers. For that reason, the water retained in boehmite samples, as proposed by Baker *et al.* for boehmite samples with a very small crystallite size (33), has another origin, which is related to the hydroxyls on a crystal surface as is explained in the following paragraph.

Boehmite crystals are thin plates with its thickness along (020) direction; therefore, most crystal surface is made of planes perpendicular to it. Because the interaction between octahedra double layers is weaker than the interaction inside the layers, crystal cleavage should occur between double layers and not inside them, producing crystal surfaces totally covered with hydroxyls bonded to aluminum atoms (Fig. 1). The oxygen atoms of these surface hydroxyls have a free orbital that give rise to the hydrogen bonds when crystals continue growing perpendicular to the surface. If crystals do not grow any more, this oxygen can react easily with atoms of an aqueous environment; when during synthesis the environment is acidic, the free orbital will react with a proton, forming an aquo ligand with an aluminum atom (35); if the environment is basic, which corresponds to the experimental condition used for the synthesis, it will form a hydrogen bonding with the hydroxyls of the environment. In this last case, a lot of weakly bonded water is formed on the crystal surface, which will be eliminated at relatively low temperatures. The above analysis explains why boehmite with a low crystallite size lost a lot of water when samples were annealed at temperatures below 200°C (14, 36) and discards the claim that pseudoboehmite is boehmite with intercalated water between the octahedra double layers (8).

Transitional Alumina Derived from Boehmite

From Al–O–OH systems, transitional aluminas are of big interest, not only from the scientific point of view (16, 37) but

also from their applications (1–4). They are characterized by having very small crystallite size and by adsorbing hydroxyls on their surface (38). Since the crystallography of these aluminas is not well known (although many authors have proposed models for it (39–41)), it is impossible to start from alumina crystallography to determine the way hydroxyls are on crystal surface. The description for boehmite surface given in the last paragraph, however, could be an alternative and realistic model for describing these hydroxyls on an alumina surface, because, like in boehmite, this surface is made only of aluminum and oxygen atoms and hydroxyls.

The transitional aluminas derived from boehmite had a crystallite size that depended on the precursor crystal dimensions: Boehmite with large (small) crystals gave rise to alumina with large (small) crystals (Table 8). The grain size of the transitional alumina was similar to the crystallite size of the precursor boehmite, because the transformation of boehmite into a transitional alumina, occurring by dehydroxylation at temperatures below 800°C, is pseudomorphic, and it involves atom displacements within only a single boehmite crystal. At higher temperatures, aluminum and oxygen atoms move between transitional alumina crystals, producing α -alumina with large crystallite dimensions. In order to get a first approximation for the crystallite size of transitional alumina, its crystalline structure was modeled with the monoclinic unit cell reported for θ -alumina (10): Atom positions have the symmetry described by space group $C2/m$. The residue obtained with this model by comparing experimental and the calculated data was 10% smaller than what one got with a nondeformed cubic unit cell having the spinel structure.

CONCLUSIONS

When boehmite precipitated at room temperature was heated between 23 and 240°C under hydrothermal conditions, its crystallite size grew between 1 and 27 nm, respectively. The Rietveld refinement of the crystalline structure revealed that boehmite bond lengths depended on crystallite

dimensions. Al–OH interaction was stronger for small crystallite sizes and the angle between these Al–OH bonds tended to a tetrahedral symmetry. The hydrogen bonding sustaining boehmite's crystalline structure and the bonding between oxygen atoms and hydroxyls inside the double layers were weaker as crystallite size decreased, which could explain why its transformation temperature into a transitional alumina also decreases with the crystallite size. Since boehmite crystals were made of plates perpendicular to [020] direction, crystal surface is full of hydroxyls interacting with water molecules, which explains the large amounts of desorbed water when samples were annealed. The crystallite size of alumina depended on boehmite crystallite size. The results of the present study suggests some tendencies about boehmite behavior, which could be verified by preparing new samples and by using additional characterization techniques; for example, the possibility that microcrystalline boehmite had a tetragonal symmetry, or that the characteristics determined for the boehmite with very small crystallite size could correspond to the behavior of boehmite or transitional alumina surface.

ACKNOWLEDGMENTS

We thank Mr. A. Morales and Mr. Manuel Aguilar for technical assistance. This work was financially supported via Grants IMP-D.01024 and IMP-D.01234.

REFERENCES

1. Z. R. Ismagilov, R. A. Shkrabina, and N. A. Koryabkina, *Catal. Today* **47**, 51 (1999).
2. J. Hietala, A. R. Root, and P. Knutila, *J. Catal.* **150**, 46 (1994).
3. F. Barath, M. Turki, V. Keller, and G. Maire, *J. Catal.* **185**, 1 (1999).
4. M. F. L. Johnson, *J. Catal.* **123**, 245 (1990).
5. J. Singh, *J. Mater. Eng. Perform.* **3**, 378 (1994).
6. A. C. Pierre, E. Elaloui, and G. M. Pajonk, *Langmuir* **14**, 66 (1998).
7. A. S. Brown, M. A. Spackman, and R. J. Hill, *Acta Crystallogr.* **49**, 513 (1993).
8. J. J. Fitzgerald, G. Piedra, S. F. Dec, M. Seger, and G. E. Maciel, *J. Am. Chem. Soc.* **119**, 7832 (1997).
9. R.-S. Zhou and R. L. Snyder, *Acta Crystallogr. B* **47**, 617 (1991).
10. E. Husson and Y. Repelin, *J. Solid State Inorg. Chem.* **33**, 1223 (1996).
11. I. Seyssiecq, S. Veesler, G. Pèpe, and R. Boistelle, *J. Cryst. Growth* **196**, 174 (1999).
12. Y. Cesteros, P. Salagre, F. Medina, and J. E. Sueiras, *Chem. Mater.* **11**, 123 (1999).
13. S. Keyser, G. K. Shter, Y. De Hazan, Y. Cohen, and G. S. Grader, *Chem. Mater.* **9**, 2464 (1997).
14. G. Chuah, S. Jaenicke, and T. H. Xu, *Microporous Mesoporous Mater.* **37**, 345 (2000).
15. M. L. Guzmán-Castillo, X. Bokhimi, A. Toledo-Antonio, J. Salmones-Blásquez, and F. Hernández-Beltrán, *J. Phys. Chem. B* **105**, 2099 (2001).
16. T. Tsukada, H. Segawa, A. Yasumori, and K. Okada, *J. Mater. Chem.* **9**, 549 (1999).
17. H.-L. Wen and F.-S. Yen, *J. Cryst. Growth* **208**, 696 (2000).
18. L. Farkas, P. Gadó, and P.-E. Werner, *Mat. Res. Bull.* **12**, 1213 (1977).
19. W. O. Milligan and J. L. McAtee, *J. Phys. Chem.* **60**, 273 (1956).

TABLE 8
Transitional-Alumina Average Crystallite Size as a Function of Boehmite Crystal Dimension

$d_{(020)}$ (nm)	d (nm)
1.13(1)	2.65(7)
1.56(2)	2.69(7)
2.04(4)	3.0(1)
2.42(4)	3.3(1)
6.90(8)	4.5(1)
14.2(2)	6.2(2)
26.3(5)	6.6(2)

20. R. A. Young, A. Sakthivel, T. S. Moss, and C. O. Paiva-Santos, *J. Appl. Crystallogr.* **28**, 366 (1995).
21. J. Rodríguez-Carbajal, Laboratoire Leon Brillouin (CEA-CNRS), France Tel: (33) 1 6908 3343, Fax: (33) 1 6908 8261, E-mail: juan@llb.saclay.cea.fr.
22. P. Thompson, D. E. Cox, and J. B. Hasting, *J. Appl. Crystallogr.* **20**, 79 (1987).
23. R. A. Young and P. Desai, *Arch. Nauki Mat.* **10**, 71 (1989).
24. E. Prince, *J. Appl. Crystallogr.* **14**, 157 (1981).
25. C. E. Corbató, R. T. Tettenhorst, and G. C. Christoph, *Clays Clay Miner.* **33**, 71 (1985).
26. X. Bokhimi, D. Acosta, M. L. Guzmán-Castillo, A. Toledo-Antonio, and F. Hernández-Beltrán, in preparation.
27. D. Chamma, Doctoral thesis, "Les résonances de Fermi en liaison hydrogène X-H...Y: profils théoriques du spectre infrarouge de l'élongation X-H." Université de Perpignan, France, 1999.
28. H. Christensen and N. Christensen, *Acta Chem. Scand. A* **32**, 87 (1978).
29. A. Olés, A. Szytula, and A. Wanic, *Phys. Status Solidi* **41**, 173 (1970).
30. A. Vázquez, T. López, R. Gómez, and X. Bokhimi, *J. Mol. Catal. A* **167**, 91 (2001).
31. L. N. Dem'yanets and A. N. Lobachev, "Crystallization Process under Hydrothermal Conditions" (A. N. Lobachev and G. D. Archard, Eds.), p. 1. Consultants Bureau, New York, 1973.
32. B. C. Lippens, "Structure and Texture of Aluminas." Doctoral thesis, Technical University of Delft, Amsterdam, 1961.
33. B. R. Baker and R. M. Pearson, *J. Catal.* **33**, 265 (1974).
34. A. De Roy, C. Forano, K. El Malki, and J. P. Besse, in "Procc. Synthesis of Microporous Materials" (M. L. Occelli and H. Robson, Eds.), Vol. 2, p. 108. Van Nostrand Reinhold, New York, 1992.
35. I. P. Kuz'mina, B. N. Litvin, and V. S. Kurazhkovskaya, in "Crystallization Process under Hydrothermal Conditions" (A. N. Lobachev and G. D. Archard, Eds.) p. 185. Consultants Bureau, New York, 1973.
36. D. L. Coke, E. D. Johnson, and R. P. Merrill, *Catal. Rev. Sci. Eng.* **26**, 163 (1984).
37. K. Sohlberg, S. J. Pennycook, and S. T. Pantelides, *J. Am. Chem. Soc.* **121**, 7493 (1999).
38. X. Liu and R. E. Truit, *J. Am. Chem. Soc.* **119**, 9856 (1997).
39. H. Knozinger and P. Ratnasamy, *Catal. Rev. Sci. Eng.* **17**, 31 (1978).
40. V. E. Henrich and P. A. Cox, "The Surface Science of Metal Oxides," Section 2.3, Cambridge Univ. Press, New York, 1994.
41. A. A. Tsyganenko and P. P. Mardilovich, *J. Chem. Soc. Faraday Trans.* **92**, 4843 (1996).